New York Journal of Mathematics

New York J. Math. **32** (2026) 1147–1170.

Geometric bounds for spanning tree entropy of planar lattice graphs

Abhijit Champanerkar and Ilya Kofman

ABSTRACT. We prove infinitely many cases of conjectured sharp upper and lower bounds for the spanning tree entropy of any planar lattice graph. These bounds come from volumes of associated hyperbolic alternating links, right-angled hyperbolic polyhedra and hyperbolic regular ideal bipyramids. For many planar lattice graphs, we show these bounds are easy to compute and provide excellent numerical estimates for the spanning tree entropy.

CONTENTS

1. Introduction

Let $\mathcal{G}$ be a connected locally finite planar biperiodic graph, which is invariant under the action of a lattice $\Lambda \cong \mathbb{Z}^2$. We will call $\mathcal{G}$ a planar lattice graph. Consider the exhaustive nested sequence of finite connected planar graphs Γ_n given by $n \times n$ copies of the Λ-fundamental domain of $\mathcal{G}$. Let $\tau(\Gamma_n)$ be the number of spanning trees of Γ_n, and let $V\Gamma_n$ be its vertex set. The *spanning tree entropy of* $\mathcal{G}$ is defined as

$$z_{\mathcal{G}} = \lim_{n\to\infty} \frac{\log \tau(\Gamma_n)}{|V\Gamma_n|}.$$

In 1973, Temperley [25] computed $z_{\mathcal{G}}$ for the square grid using a bijection between spanning trees and dimer coverings (perfect matchings). Temperley's

Received June 18, 2025.

2020 *Mathematics Subject Classification.* 57K32, 05C10, 57K10, 11R06.

Key words and phrases. spanning tree entropy, hyperbolic volume, alternating link, Mahler measure, orthogonally dual graphs.

The research of both authors is partially supported by grants from the Simons Foundation and PSC-CUNY.

ISSN 1076-9803/2026

bijection has been extended in many ways to compute $z_{\mathcal{G}}$ in more general settings (see, e.g., [20, 21]). For planar lattice graphs, $z_{\mathcal{G}}$ is sometimes exactly computable using its quotient graph on the torus (see, e.g., [7, 20, 23]).

A surprising fact about $z_{\mathcal{G}}$ for many planar lattice graphs is that its value is closely related to hyperbolic geometry. Let $v_{\text{tet}} \approx 1.01494$ be the volume of the hyperbolic regular ideal tetrahedron, and $v_{\text{oct}} \approx 3.66386$ be the volume of the hyperbolic regular ideal octahedron. If $\mathcal{G}_{\triangle}$, $\mathcal{G}_{\square}$ and $\mathcal{G}_{\hexagon}$ denote the regular triangular, square and hexagonal lattice graphs, then

$$2\pi\, z_{\mathcal{G}_{\triangle}} = 10v_{\text{tet}}, \qquad 2\pi\, z_{\mathcal{G}_{\square}} = 2v_{\text{oct}}, \qquad 2\pi\, z_{\mathcal{G}_{\hexagon}} = 5v_{\text{tet}}.$$

See, e.g., [7, Theorems 12, 13]; see Section 5 for another proof. In Conjecture 1.1 below, we propose upper and lower bounds for $z_{\mathcal{G}}$ for any planar lattice graph $\mathcal{G}$. The volume of an associated hyperbolic link provides the lower bound, which is sharp for the regular planar lattice graphs.

There is a well-known correspondence between alternating link diagrams and planar graphs: If the faces of the link diagram are checkerboard colored, the *Tait graph* is the planar graph for which a vertex is assigned to every shaded region and an edge to every crossing of the link diagram. Using the other checkerboard coloring yields the dual graph. Conversely, the medial graph of any planar graph (or its dual) is the projection graph of an alternating link diagram.

Similarly, a planar lattice graph $\mathcal{G}$ is the Tait graph of a *biperiodic alternating link* $\mathcal{L}$ in $\mathbb{R}^2 \times I$. Then $G = \mathcal{G}/\Lambda$ is a graph on the torus T^2, which is the Tait graph of an alternating link diagram on T^2. Let L be the link in the thickened torus $T^2 \times I$, such that $L = \mathcal{L}/\Lambda$. Let G^* be the dual graph of G on T^2. Let VG, EG, FG denote the sets of vertices, edges and faces of G. If G and G^* are 2-connected and their faces are topologically disks on the torus, then $(T^2 \times I) - L$ is a complete finite-volume hyperbolic 3–manifold [17, Theorem 4.2]. Moreover, the crossing number $c(L) = |EG|$ is minimal among all toroidal diagrams of L [2]. Using its hyperbolic volume, we define

$$\text{vol}(G) = \text{vol}((T^2 \times I) - L) \quad \text{and} \quad \text{vol}(\mathcal{G}) = \frac{\text{vol}(G)}{|VG|} \quad \text{and} \quad \overline{\nu}(\mathcal{G}) = \frac{|EG| v_{\text{oct}}}{|VG|}.$$

Conjecture 1.1.

$$\text{vol}(\mathcal{G}) \;\leq\; 2\pi\, z_{\mathcal{G}} \;\leq\; \overline{\nu}(\mathcal{G}).$$

Conjecture 1.1 lies at the intersection of hyperbolic geometry, number theory, probability and graph theory. In this paper, we explain the context and provide numerical evidence for Conjecture 1.1, and we prove infinitely many cases of Conjecture 1.1. Most of the results proved in this paper address the lower bound in Conjecture 1.1. The hyperbolic volume of a link can be computed numerically using the computer program SnapPy [11]. Finding the spanning tree entropy of a planar lattice graph involves laborious computations and many recent published papers just compute examples. Finding exact values for both quantities is far more difficult, and when possible requires advanced techniques from number theory; see e.g., [7]. Instead, below we define several new

geometric invariants associated to planar graphs and lattice graphs that are easier to compute, are numerically very close to the spanning tree entropy in many examples, and are easier to study asymptotically.

In Section 2, we define the bipyramid volume $\nu^{\Diamond}(\mathcal{G})$ of a planar lattice graph $\mathcal{G}$, and we show

$$0 \;<\; \mathrm{vol}(\mathcal{G}) \;\leq\; \nu^{\Diamond}(\mathcal{G}).$$

If $\nu^{\Diamond}(\mathcal{G}) \leq 2\pi\, z_{\mathcal{G}}$, then $\mathrm{vol}(\mathcal{G}) \leq 2\pi\, z_{\mathcal{G}}$, as in Conjecture 1.1. The bipyramid volume is easier to compute than $\mathrm{vol}(\mathcal{G})$ or $z_{\mathcal{G}}$, and we show for 16 planar lattice graphs that it provides both a lower bound and an excellent estimate for $z_{\mathcal{G}}$. We also show that for one planar lattice graph, the bipyramid volume is not a lower bound for $z_{\mathcal{G}}$, which contradicts [7, Conjecture 1]. This exceptional planar lattice graph still satisfies Conjecture 1.1.

In Section 3, we recall the Vol-Det Conjecture [8, Conjecture 1.10] from hyperbolic knot theory, which is that for any alternating hyperbolic link K,

$$\mathrm{vol}(K) < 2\pi\, \log \det(K).$$

We present strict inequalities for finite alternating links that extend to the sharp inequalities for biperiodic alternating links in Conjecture 1.1. Namely, we define the volume and bipyramid volume for a finite planar graph, and we state Conjecture 3.2, which gives similar geometric bounds for the number of spanning trees of finite planar graphs. For finite planar graphs that asymptotically converge to the planar lattice graph $\mathcal{G}$, their bipyramid volumes converge to that of $\mathcal{G}$. We show that whenever the bipyramid volume of $\mathcal{G}$ is a lower bound for $z_{\mathcal{G}}$ with a strict inequality, we obtain infinitely many finite planar graphs converging to $\mathcal{G}$ that satisfy Conjecture 3.2, which provide infinite families of alternating links that satisfy the Vol-Det Conjecture.

In Section 4, we apply another useful property of the bipyramid volume, that its logarithmic growth rate is similar to that of $z_{\mathcal{G}}$. We prove Conjecture 1.1 for infinitely many cases using three different ways to obtain infinite families of planar lattice graphs: by inserting parallel edges, by truncating any 3-regular planar lattice graph, and by taking the medial graph of a 3-regular planar lattice graph. The bipyramid volume provides a lower bound for $z_{\mathcal{G}}$ in all of these infinitely many cases. Previously, in [7], it was proved that the bipyramid volume provides a lower bound for $z_{\mathcal{G}}$ for six biperiodic alternating links using rigorous computations for the Mahler measures of the corresponding 2-variable polynomials. In [16], four other lower bounds were proved using methods from graph theory in [26].

In Section 5, we define another geometric invariant of a planar lattice graph $\mathcal{G}$, the volume of an associated hyperbolic right-angled polyhedron, which we call the right-angled volume $\mathrm{vol}^{\perp}(\mathcal{G})$. If $\mathcal{G}$ and $\mathcal{G}^*$ satisfy a geometric condition called orthogonal duality, then

$$\mathrm{vol}^{\perp}(\mathcal{G}) \;\leq\; \mathrm{vol}(\mathcal{G}) \;\leq\; \nu^{\Diamond}(\mathcal{G}).$$

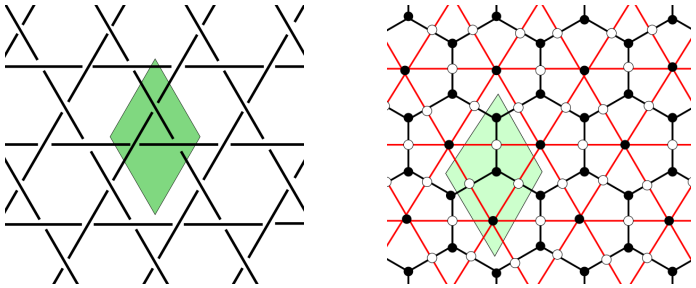

(a) (b)

FIGURE 1. (a) Biperiodic triaxial link $\mathcal{L}$, and fundamental domain for L. (b) Temperleyan graph $\mathcal{G}^b$, and fundamental domain for G^b.

Thus, Conjecture 1.1 implies $\text{vol}^{\perp}(\mathcal{G}) \leq 2\pi\, z_{\mathcal{G}}$, and we show that $\text{vol}^{\perp}(\mathcal{G})$ is exactly computable using the local geometry of G. The three regular planar lattice graphs satisfy both isoradiality and orthogonal duality, which we exploit using the isoradial dimer model to prove that the lower bound in Conjecture 1.1 holds with equality for these lattice graphs.

Acknowledgement. We thank Hong-Chuan Gan for stimulating discussions.

2. Bipyramid volume of a planar lattice graph

Finding numerical values for the spanning tree entropy of a planar lattice graph involves laborious computations, and exact values are usually difficult to prove (see [7]). Instead, below we define the bipyramid volume, which can be easily computed for a planar lattice graph. If the bipyramid volume is a lower bound for $z_{\mathcal{G}}$, then the lower bound in Conjecture 1.1 holds for $\mathcal{G}$. As we show in many examples, the bipyramid volume is also an excellent estimate for the spanning tree entropy. However, in Section 2.2, we show that it does not always provide a lower bound.

Let G and G^* be dual 2-connected graphs embedded on the torus, such that their faces are topologically disks, and each edge of G intersects its dual edge exactly once and does not intersect any other edge of G^*. Let $\mathcal{G}$ be the biperiodic graph in $\mathbb{R}^2$, such that $G = \mathcal{G}/\Lambda$ for Λ as above. These conditions will be assumed for all graphs and lattice graphs below.

We form the *Temperleyan graph* G^b on the torus as follows: The black vertices of G^b are the vertices of G and of G^*; the white vertices of G^b are the intersections of edges of G and of G^*. The edges of G^b join a black vertex for each face of G and of G^* to every white vertex incident to the face, so that G^b is a balanced bipartite graph. Let $\mathcal{G}^b$ be the biperiodic bipartite graph, such that $G^b = \mathcal{G}^b/\Lambda$. See Figure 1.

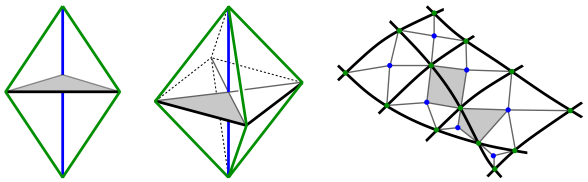

(a) (b) (c)

FIGURE 2. (a) A tetrahedron with stellating (blue), vertical (green), and horizontal (black) edges. A link triangle for an ideal vertex at ∞ is shaded. (b) Tetrahedra are glued at the stellating edge, centrally triangulating faces of G on the torus. (c) Shaded triangles indicate the four tetrahedra glued along one horizontal edge.

Right: Volumes of hyperbolic regular ideal n-bipyramids.

n	$\mathrm{vol}(B_n)$
2	0
3	2.02988
4	3.66386
5	4.98677
6	6.08965
7	7.03257
8	7.85498
9	8.58367
10	9.23755
11	9.83040
12	10.37255
13	10.87192
14	11.33474
15	11.76597
20	13.56682
100	23.67095
1,000	38.13817
1,000,000	81.5409

Definition 2.1. *Let B_n denote the hyperbolic regular ideal bipyramid whose link polygons at the two coning vertices are regular n–gons. The hyperbolic volume of B_n is given by*

$$\mathrm{vol}(B_n) = 2n\, L(\pi/n), \quad \text{for } L(\theta) = -\int_0^\theta \log|2\sin t|\, dt,$$

where $L(\theta)$ is the Lobachevsky function. Since B_3 consists of two regular ideal tetrahedra and B_4 is the hyperbolic regular ideal octahedron,

$$\mathrm{vol}(B_3) = 2v_{\mathrm{tet}} \approx 2.02988 \quad \text{and} \quad \mathrm{vol}(B_4) = v_{\mathrm{oct}} \approx 3.66386.$$

We allow $n = 2$, but note $\mathrm{vol}(B_2) = 0$. For $n \geq 3$, $\mathrm{vol}(B_n) < 2\pi\log(n/2)$ and grows asymptotically like $2\pi\log(n/2)$ [1]. See the table of values of $\mathrm{vol}(B_n)$ in Figure 2 (Right), which is adapted from [1].

For $v \in VG$ and $f \in FG$, let $|v|$ and $|f|$ denote their degree; i.e., the number of incident edges. Define the bipyramid volume *of a toroidal graph G as*

$$\mathrm{vol}^{\Diamond}(G) = \sum_{f\in FG} \mathrm{vol}(B_{|f|}).$$

Proposition 2.2. $0 < \mathrm{vol}(G) \leq \mathrm{vol}^{\Diamond}(G) + \mathrm{vol}^{\Diamond}(G^*)$.

Proof. This is essentially proved in the last part of [9, Theorem 7.5], and the extra condition in that theorem is not required for this part. Our conditions on G ensure that $(T^2 \times I) - L$ is hyperbolic, and that after collapsing bigons if needed, $(T^2 \times I) - L$ admits an ideal, positively oriented triangulation [9,

Lemma 2.5]. (In Section 5, we add conditions for this hyperbolic structure to be right-angled.) Thus, $\mathrm{vol}(G) > 0$.

By [9, Lemma 2.6], the ideal tetrahedra in this triangulation can be combined around every stellating edge as in Figure 2 to form a hyperbolic ideal bipyramid over each face of L. Since the projection of L is the medial graph of G, these are exactly the faces of G and of G^*. By [1], the maximal volume of hyperbolic bipyramids is achieved by the regular bipyramids, whose volumes sum to $\mathrm{vol}^{\Diamond}(G) + \mathrm{vol}^{\Diamond}(G^*)$. □

Definition 2.3. *Let $z_G^{\mathrm{fd}} = |VG| z_{\mathcal{G}}$, which is the spanning tree entropy per fundamental domain of $\mathcal{G}$. The spanning tree entropy per vertex, rather than per fundamental domain, is usually computed. To bound $z_{\mathcal{G}}$, we define the* bipyramid volume of $\mathcal{G}$ *as follows:*

$$\nu^{\Diamond}(\mathcal{G}) = \frac{\mathrm{vol}^{\Diamond}(G) + \mathrm{vol}^{\Diamond}(G^*)}{|VG|}.$$

All faces of G^b are quads, and $|FG^b| = 2|EG|$, so $\mathrm{vol}^{\Diamond}(G^b) = |FG^b|\mathrm{vol}(B_4) = 2|EG|v_{\mathrm{oct}}$. Thus,

$$\overline{\nu}(\mathcal{G}) = \frac{|EG|v_{\mathrm{oct}}}{|VG|} = \frac{\mathrm{vol}^{\Diamond}(G^b)}{2|VG|}.$$

Proposition 2.4. *If $\mathcal{G}$ satisfies the following inequalities in (1), then Conjecture 1.1 holds for $\mathcal{G}$.*

$$\mathrm{vol}^{\Diamond}(G) + \mathrm{vol}^{\Diamond}(G^*) \le 2\pi\, z_G^{\mathrm{fd}} \le |EG|v_{\mathrm{oct}} \iff \nu^{\Diamond}(\mathcal{G}) \le 2\pi\, z_{\mathcal{G}} \le \overline{\nu}(\mathcal{G}). \quad (1)$$

Proof. By Proposition 2.2, $0 < \mathrm{vol}(\mathcal{G}) \le \nu^{\Diamond}(\mathcal{G})$. □

We use Proposition 2.4 to prove Conjecture 1.1 for infintely many planar lattice graphs in Section 4. However, in Section 2.2 we discuss a planar lattice graph for which Conjecture 1.1 holds, but which does not satisfy the lower bound in (1).

As mentioned above, for the regular triangular, square and hexagonal lattice graphs,

$$\nu^{\Diamond}(\mathcal{G}_{\triangle}) = 2\pi\, z_{\mathcal{G}_{\triangle}} = 10v_{\mathrm{tet}}, \quad \nu^{\Diamond}(\mathcal{G}_{\square}) = \overline{\nu}(\mathcal{G}_{\square}) = 2\pi\, z_{\mathcal{G}_{\square}} = 2v_{\mathrm{oct}}$$

$$\nu^{\Diamond}(\mathcal{G}_{\hexagon}) = 2\pi\, z_{\mathcal{G}_{\hexagon}} = 5v_{\mathrm{tet}}.$$

Hence, the lower bound in Conjecture 1.1 is sharp for $\mathcal{G}_{\triangle}$, $\mathcal{G}_{\square}$, $\mathcal{G}_{\hexagon}$, and the upper bound is sharp for $\mathcal{G}_{\square}$; see, e.g., [7, Theorems 12, 13].

Question 2.5. *Is there a planar lattice graph $\mathcal{G}$, other than $\mathcal{G}_{\triangle}$, $\mathcal{G}_{\square}$, $\mathcal{G}_{\hexagon}$, for which $\nu^{\Diamond}(\mathcal{G}) = 2\pi\, z_{\mathcal{G}}$? Is there a planar lattice graph $\mathcal{G}$, other than $\mathcal{G}_{\square}$, for which $\overline{\nu}(\mathcal{G}) = 2\pi\, z_{\mathcal{G}}$?*

The Tait graphs for the square weave and the triaxial link as in Figure 1 are $\mathcal{G}_{\triangle}$, $\mathcal{G}_{\square}$, $\mathcal{G}_{\hexagon}$. Question 2.5 asks whether these are the only two biperiodic alternating links, such that $\mathrm{vol}^{\Diamond}(G) + \mathrm{vol}^{\Diamond}(G^*) = 2\pi\, z_G^{\mathrm{fd}}$; and whether the square

Planar lattice graph $\mathcal{G}$	$\lvert VG\rvert$	$\nu^{\diamondsuit}(\mathcal{G})/2\pi$	$z_{\mathcal{G}}$	$\overline{\nu}(\mathcal{G})/2\pi$
1. Triangular (3^6)	1	1.61533	1.61533	1.74937
2. Square (4^4)	1	1.16624	1.16624	1.16624
3. Hexagonal (6^3)	2	0.80766	0.80766	0.87468
4. Kagome (3-6-3-6)	3	1.12157	1.13570	1.16624
5. Square-octagon (4-8-8)	4	0.78139	0.78668	0.87468
6. Medial(4-8-8)	6	1.10405	1.12171	1.16624
7. 3-12-12	6	0.70590	0.72056	0.87468
8. 3-4-6-4	6	1.14390	1.14480	1.16624
9. 4-6-12	12	0.76795	0.77780	0.87468
10. Cairo pentagonal lattice graph	6	0.93886	0.94057	0.97187
11. Lattice graph in Figure 4	9	0.84361	0.84744	0.90708
12. Lattice graph #12 in Figure 3	3	1.07689	1.10365	1.16624
13. Lattice graph #13 in Figure 3	2	1.39079	1.39928	1.74937
14. 3^2-4-3-4	4	1.40830	1.41086	1.45780
15. 4^4; 3^3-4^2	3	1.32761	1.32772	1.36062
16. 3^6; 3^3-4^2	3	1.47731	1.47732	1.55499

TABLE 1. Geometric bounds for $z_{\mathcal{G}}$ for 16 planar lattice graphs. See Figures 3, 4 and 6 for pictures of the planar lattice graphs.

weave is the only one such that $2\pi\, z_G^{\mathrm{fd}} = |EG|v_{\mathrm{oct}}$ (see [7, 8]). Question 2.5 seems related to [18, Corollary 20], which established that the square weave and the triaxial link are the only semi-regular links with certain geometric properties, but these properties may not be required for these equalities to hold.

2.1. Examples. In Table 1, we show that $\nu^{\diamondsuit}(\mathcal{G}) \le 2\pi\, z_{\mathcal{G}} \le \overline{\nu}(\mathcal{G})$ holds for 16 planar lattice graphs. Therefore, Conjecture 1.1 holds for these lattice graphs, and infinitely many other lattice graphs using results in Section 4. The values in each column for lattice graphs #1-7 and 12-13 are known by exact computations, and equal values in Table 1 indicate exact equality (see [7]). For the remaining lattice graphs, $z_{\mathcal{G}}$ is computed numerically (see Problem 2.7). Below, we discuss each of these examples.

1-3. For the regular lattice graphs, the equal values in the table are exactly equal.
4. The kagome lattice graph is the medial graph of the hexagonal lattice graph, as in Theorem 4.4.
5. Exact values for the square-octagon lattice graph are computed in [7, Theorem 19].
6. This lattice graph is the medial graph of the square-octagon lattice graph, as in Theorem 4.4.

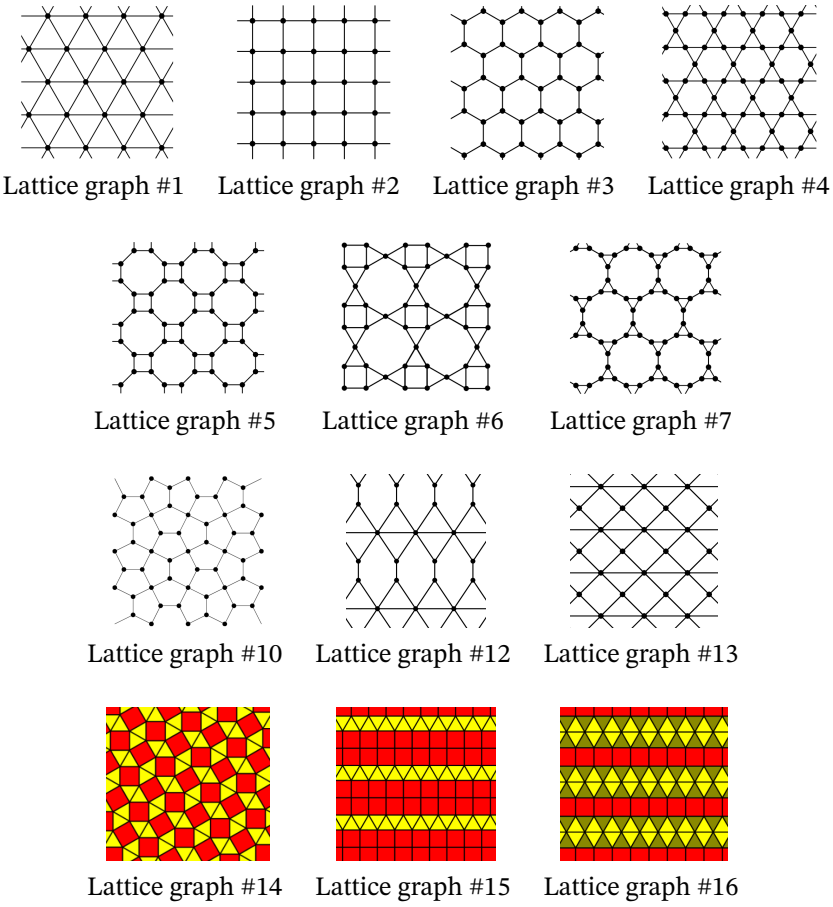

FIGURE 3. Some planar lattice graphs in Table 1. Figures for Lattice graphs #1-5 and 7 are from [26]. Figures for Lattice graphs #14-16 are from [24]. For Lattice graphs #8-9, see Figure 6. For Lattice graph #11, see Figure 4.

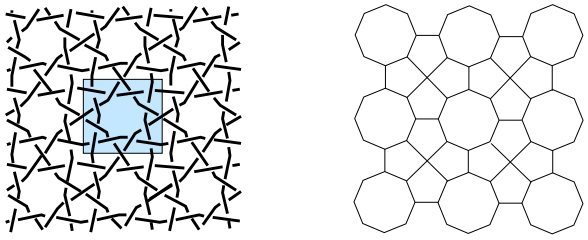

FIGURE 4. Biperiodic alternating link whose Tait graph is Lattice graph #11 in Table 1.

7. The 3-12-12 lattice graph is the truncation of the hexagonal lattice graph, as in Theorem 4.3.

8. The 3-4-6-4 lattice graph is the medial graph of the kagome lattice graph. Its numerical $z_{\mathcal{G}}$ value is computed in [10, Section 3.4].
9. The numerical $z_{\mathcal{G}}$ value for this lattice graph is computed in [10, Section 3.5].
10. The numerical $z_{\mathcal{G}}$ value for this lattice graph is computed in [22, Corollary 2.2].
11. This lattice graph is the Tait graph of the link shown in Figure 4, and its $z_{\mathcal{G}}$ value is computed numerically in [7, Section 1.4].
12. Exact values for this lattice graph are computed in [7, Theorem 15].
13. Exact values for this lattice graph are computed in [7, Theorem 17].
14. This lattice graph is the dual of Lattice graph #10.

15-16. We computed the numerical $z_{\mathcal{G}}$ values using the methods in [7]; see Problem 2.7.

2.2. Non-example. Let $\mathcal{G}$ be the 3^3-4^2 lattice graph, which is shown in Figure 5 below. Using the methods discussed in [7], we computed the characteristic polynomial $p(z,w)$ of the toroidal dimer model for $\mathcal{G}$:

$$p(z,w) = -wz^4 + w^2z^2 + 11wz^3 + w^2z - 24wz^2 + z^3 + 11wz + z^2 - w.$$

The Mahler measure $\mathrm{m}(p(z,w)) = z_G^{\mathrm{fd}}$ by [20], as explained in [6, Proposition 5.3].

Conjecture 1 of [7] would imply that $\mathrm{vol}^{\diamondsuit}(G) + \mathrm{vol}^{\diamondsuit}(G^*) \leq 2\pi\,\mathrm{m}(p(z,w))$. However, we numerically computed $\mathrm{m}(p(z,w))$, and $\mathrm{vol}((T^2 \times I) - L)$ using Snappy [11]:

$$\begin{array}{ccccccc} \mathrm{vol}((T^2\times I)-L) & < & 2\pi\,\mathrm{m}(p(z,w)) & < & \mathrm{vol}^{\diamondsuit}(G)+\mathrm{vol}^{\diamondsuit}(G^*) & < & |EG|v_{\mathrm{oct}} \\ 17.55732 & < & 17.67995 & < & 17.69718 & < & 18.31931 \end{array}$$

Therefore, $\mathcal{G}$ does not satisfy the lower bound in (1). The biperiodic alternating link $\mathcal{L}$ whose Tait graph is $\mathcal{G}$ is a counterexample to [7, Conjecture 1]. Nevertheless, $\mathcal{G}$ satisfies Conjecture 1.1.

In contrast to the examples in Table 1, this case has (with $|VG| = 2$):

$$\begin{array}{ccccccccc} & \mathrm{vol}(\mathcal{G}) & < & 2\pi\, z_{\mathcal{G}} & < & \nu^{\diamondsuit}(\mathcal{G}) & < & \overline{\nu}(\mathcal{G}) & \\ 2\pi * (& 1.39717 & < & 1.40693 & < & 1.40830 & < & 1.45780 &) \end{array}$$

The numerical $z_{\mathcal{G}}$ value is also computed in [10, Section 3.1]. We do not know any other counterexamples to [7, Conjecture 1]. The above figure from [24] suggests that $\mathcal{G}$ is similar to Lattice graphs #14-16 in Table 1, but for these lattice graphs $\nu^{\diamondsuit}(\mathcal{G}) < 2\pi\, z_{\mathcal{G}}$, although their values of $\nu^{\diamondsuit}(\mathcal{G})$ and $2\pi\, z_{\mathcal{G}}$ are very close! Adding parallel edges to any of these four lattice graphs, as in Theorem 4.2 below, also results in lattice graphs $\mathcal{G}$ with $\nu^{\diamondsuit}(\mathcal{G}) < 2\pi\, z_{\mathcal{G}}$.

Question 2.6. *For which other planar lattice graphs is* $2\pi\, z_{\mathcal{G}} < \nu^{\Diamond}(\mathcal{G})$*?*

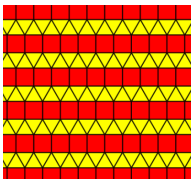

FIGURE 5. Lattice graph 3^3-4^2

Problem 2.7. The inequalities $\mathrm{vol}(\mathcal{G}) < 2\pi\, z_{\mathcal{G}}$ for the non-example above and lattice graphs #8, 9, 10, 11, 14, 15, 16 in Table 1 are not proved by exact computations. In principle, using $z_G^{\mathrm{fd}} = \mathrm{m}(p(z,w))$, we can prove each inequality $\mathrm{vol}((T^2 \times I) - L) < 2\pi\, \mathrm{m}(p(z,w))$ rigorously by interval arithmetic; e.g., using ComplexBallField (CBF) in SageMath. However, for sufficiently high precision, we could not rigorously compute $\mathrm{m}(p(z,w))$ in a reasonable time. Problem 2.7 is to rigorously prove $\mathrm{vol}(\mathcal{G}) < 2\pi\, z_{\mathcal{G}}$ for these lattice graphs. For lattice graphs #15, 16, polynomials $p(z,w)$ are as follows:

Lattice graph	Polynomial $p(z,w)$
#15	$p(z,w) = -wz^6 + 15wz^5 + w^2z^3 - 68wz^4 + w^2z^2$
	$+ 112wz^3 + z^4 - 68wz^2 + z^3 + 15wz - w$
#16	$p(z,w) = -wz^6 - w^2z^4 + 18wz^5 - 2w^2z^3 - 93wz^4 - w^2z^2$
	$+ 160wz^3 - z^4 - 93wz^2 - 2z^3 + 18wz - z^2 - w$

3. Finite planar graphs

For a finite connected graph Γ, the number of spanning trees $\tau(\Gamma)$ is an important measure of its complexity. For finite planar graphs, many interesting bounds are known (see, e.g., [4]), and asymptotic enumeration of spanning trees by finite planar graphs that approach a planar lattice graph is sometimes exactly computable (see, e.g., [7, 20, 23]).

Any finite connected planar graph Γ is the Tait graph of an alternating link K in S^3, so the link diagram of K projects to the medial graph of Γ. We define

$$\mathrm{vol}(\Gamma) = \mathrm{vol}(S^3 - K),$$

$$\mathrm{vol}^{\Diamond}(\Gamma) = \sum\nolimits_{f \in \{\substack{\text{bounded}\\ \text{faces of}\ \Gamma}\}} \mathrm{vol}(B_{|f|}) \quad \text{and} \quad \nu^{\Diamond}(\Gamma) = \frac{\mathrm{vol}^{\Diamond}(\Gamma) + \mathrm{vol}^{\Diamond}(\Gamma^*)}{|V\Gamma|}.$$

Proposition 3.1. *If neither* Γ *nor* Γ^* *has loops or a cut-vertex, and neither is a cycle graph, then*

$$0 \;<\; \mathrm{vol}(\Gamma) \;<\; \mathrm{vol}^{\Diamond}(\Gamma) + \mathrm{vol}^{\Diamond}(\Gamma^*).$$

Proof. The alternating diagram is reduced if neither Γ nor Γ^* has loops. The alternating link K is prime if neither Γ nor Γ^* has a cut-vertex. By the classification of hyperbolic alternating links due to Thurston and Menasco, K is hyperbolic with finite volume if it is reduced, prime and not a $(2,n)$-torus link.

With our conditions, K is hyperbolic with finite volume if neither Γ nor Γ^* is a cycle graph. Thus, $\mathrm{vol}(\Gamma) > 0$. Since the projection of K is the medial graph of Γ, the faces of K are exactly the faces of Γ and of Γ^*. Hence, our conditions on Γ satisfy those in [1, Theorem 4.1], which implies the strict upper bound. □

We conjecture the following geometric bounds for the number of spanning trees of a finite connected planar graph:

Conjecture 3.2. *If* $\mathrm{vol}(\Gamma) > 0$ *then*

$$\mathrm{vol}(\Gamma) < 2\pi \log \tau(\Gamma) < |E\Gamma| v_{\mathrm{oct}}.$$

Conjecture 3.2 is a restatement of [8, Conjectures 1.1 and 1.10]. The conjectured upper bound $|EG|v_{\mathrm{oct}}$ is essentially due to Kenyon; see [8, Conjecture 2.3] for more details.

The lower bound, called the Vol-Det Conjecture, has been verified for all hyperbolic alternating knots with up to 16 crossings, i.e., $|E\Gamma| \leq 16$, as well as all 2-bridge links and alternating 3-braids in [5], and highly twisted alternating links in [14]. Moreover, the constant 2π cannot be improved in the lower bound: By [8, Corollary 1.11], if $\alpha < 2\pi$, then there exist hyperbolic alternating knots K, such that $\alpha \log \tau(\Gamma) < \mathrm{vol}(\Gamma)$.

Theorem 3.3. *Let* $\mathcal{G}$ *be a planar lattice graph that satisfies*

$$\mathrm{vol}^{\Diamond}(G) + \mathrm{vol}^{\Diamond}(G^*) \;<\; 2\pi\, z_G^{\mathrm{fd}} \;<\; |EG| v_{\mathrm{oct}}.$$

Let Γ_n *be a sequence of connected planar graphs with bounded average degree that converges to* $\mathcal{G}$ *as in* [23, Theorem 3.2]. *Then for all but finitely many* n,

$$\mathrm{vol}(\Gamma_n) \;<\; 2\pi \log \tau(\Gamma_n) \;<\; |E\Gamma_n| v_{\mathrm{oct}}.$$

Proof. By [7, Theorem 8], $\nu^{\Diamond}(\Gamma)$ behaves well under the type of convergence as in [23, Theorem 3.2]; namely,

$$\Gamma_n \to \mathcal{G} \quad \Rightarrow \quad \lim_{n\to\infty} \nu^{\Diamond}(\Gamma_n) = \nu^{\Diamond}(\mathcal{G}).$$

Thus, the lower bound is a restatement of [7, Theorem 3]. For the upper bound, the convergence is similar: $|E\Gamma_n|/|V\Gamma_n| \to |EG|/|VG|$. □

Thus, whenever the inequalities in (1) are strict inequalities for a planar lattice graph, we obtain infinitely many planar graphs that satisfy Conjecture 3.2.

4. Infinitely many proven cases for Conjecture 1.1

In this section, we use three different ways to construct infinite families of planar lattice graphs that are proven cases for Conjecture 1.1 using bipyramid volume in an essential way. Namely, we prove that these planar lattice graphs satisfy the inequalities in (1), so Proposition 2.4 implies Conjecture 1.1 for $\mathcal{G}$.

4.1. Parallel edges. For any planar lattice graph $\mathcal{G}$, let $\mathcal{G}_s$ denote the planar lattice graph for which every edge of $\mathcal{G}$ is replaced by s parallel edges. Then (see [26])

$$z_{\mathcal{G}_s} = z_{\mathcal{G}} + \log s.$$

In Theorem 4.2, we show that if the inequalities in (1) hold for $\mathcal{G}$, then they hold with strict inequalities for $\mathcal{G}_s$ for any $s \geq 2$.

Lemma 4.1. *Fix an integer $s \geq 2$. Then for all $n \geq 2$,*

$$\mathrm{vol}(B_{ns}) - \mathrm{vol}(B_n) < 2\pi \log s.$$

Proof. We can modify the proof of [1, Theorem 2.2]. Decompose B_n into n isometric ideal tetrahedra T_n, such that each T_n intersects the stellating edge of B_n with an edge of dihedral angle $2\pi/n$, as in Figure 2(a,b). Thus, $\mathrm{vol}(B_n) = n \cdot \mathrm{vol}(T_n)$.

$$\mathrm{vol}(B_{ns}) < \mathrm{vol}(B_n) + 2\pi \log s \quad \Longleftrightarrow \quad \mathrm{vol}(T_{ns}) < \frac{1}{s}\mathrm{vol}(T_n) + \frac{1}{ns} 2\pi \log s.$$

Let $f(n) = \mathrm{vol}(T_{ns})$ and $g(n) = \frac{1}{s}\mathrm{vol}(T_n) + \frac{1}{ns} 2\pi \log s$. We must prove that $f(n) < g(n)$ for all $n \geq 2$. By [1, Theorem 2.2], $f(2) < g(2)$ and the functions f and g agree asymptotically as $n \to \infty$. If $f(a) > g(a)$ for some $a > 2$, then it must be true that $f'(b) < g'(b)$ for some $b > a$. But we now prove that $f'(x) > g'(x)$ for all $x \geq 2$.

$$f'(n) = \frac{2\pi}{n^2 s} \log\left(2 \sin\left(\frac{\pi}{ns}\right)\right)$$

$$g'(n) = \frac{2\pi}{n^2 s} \log\left(2 \sin\left(\frac{\pi}{n}\right)\right) - \frac{2\pi}{n^2 s} \log s = \frac{2\pi}{n^2 s} \log\left(\frac{2}{s} \sin\left(\frac{\pi}{n}\right)\right).$$

Since $h(\theta) = \dfrac{\sin\theta}{\theta}$ is a decreasing function for $0 < \theta < \pi$, then $\dfrac{\sin(\pi/ns)}{\pi/ns} > \dfrac{\sin(\pi/n)}{\pi/n}$ for any $s \geq 2$. Thus,

$$\sin\left(\frac{\pi}{ns}\right) > \frac{1}{s} \sin\left(\frac{\pi}{n}\right).$$

Therefore, $f'(x) > g'(x)$ for all $x \geq 2$. This implies that for all $n \geq 2$, $f(n) < g(n)$. □

Theorem 4.2. *Let $s \geq 2$. If $\nu^{\Diamond}(\mathcal{G}) \leq 2\pi\, z_{\mathcal{G}} \leq \overline{\nu}(\mathcal{G})$, then*

$$\nu^{\Diamond}(\mathcal{G}_s) < 2\pi\, z_{\mathcal{G}_s} < \overline{\nu}(\mathcal{G}_s).$$

Proof. We first prove the lower bound. Every face $f \in FG$ with $|f| > 2$ has the same degree in G_s, and $\mathrm{vol}(B_2) = 0$, so

$$\mathrm{vol}^{\Diamond}(G) + \mathrm{vol}^{\Diamond}(G^*) = \sum\nolimits_{f \in FG} \mathrm{vol}(B_{|f|}) + \sum\nolimits_{v \in VG} \mathrm{vol}(B_{|v|}),$$

$$\mathrm{vol}^{\Diamond}(G_s) + \mathrm{vol}^{\Diamond}(G_s^*) = \sum\nolimits_{f\in FG} \mathrm{vol}(B_{|f|}) + \sum\nolimits_{v\in VG} \mathrm{vol}(B_{s|v|}).$$

Then by Lemma 4.1,

$$\mathrm{vol}^{\Diamond}(G_s^*) - \mathrm{vol}^{\Diamond}(G^*) \le |VG| \max_{v\in VG} \big(\mathrm{vol}(B_{s|v|}) - \mathrm{vol}(B_{|v|})\big) < 2\pi |VG| \log s.$$

Dividing by $|VG|$, this implies $\nu^{\Diamond}(\mathcal{G}_s) < \nu^{\Diamond}(\mathcal{G}) + 2\pi \log s$. Since we assumed $\nu^{\Diamond}(\mathcal{G}) \le 2\pi\, z_{\mathcal{G}}$, then $\nu^{\Diamond}(\mathcal{G}_s) < 2\pi\, z_{\mathcal{G}} + 2\pi \log s = 2\pi\, z_{\mathcal{G}_s}$.

We now prove the upper bound, assuming $2\pi\, z_{\mathcal{G}} \le \overline{\nu}(\mathcal{G})$. Since $|EG_s| = s|EG|$, we have

$$\begin{aligned} z^{\mathrm{fd}}_{G_s} = z^{\mathrm{fd}}_{G} + \log s &\le \frac{|EG|v_{\mathrm{oct}}}{2\pi} + \log s \\ &= \frac{1}{s}\left(\frac{s|EG|v_{\mathrm{oct}}}{2\pi} + s\log s\right) \\ &< \frac{1}{s}\left(\frac{|EG_s|v_{\mathrm{oct}}}{2\pi} + \frac{(s-1)|EG_s|v_{\mathrm{oct}}}{2\pi}\right) \\ &= \frac{|EG_s|v_{\mathrm{oct}}}{2\pi} \\ 2\pi\, z_{\mathcal{G}_s} &< \overline{\nu}(\mathcal{G}_s). \end{aligned}$$

The strict inequality follows because for any $s \ge 2$,

$$\frac{2\pi \log s}{(s-1)v_{\mathrm{oct}}} < 2 < |EG|.$$

□

4.2. Truncating a 3-regular planar lattice graph. For any 3-regular planar lattice graph $\mathcal{G}$, let $\mathcal{G}'$ denote the lattice graph for which every vertex is replaced by a triangle (i.e., complete graph K_3), and each edge of $\mathcal{G}$ is preserved in $\mathcal{G}'$. For example, the 3-12-12 lattice graph is obtained by truncating the regular hexagonal lattice graph:

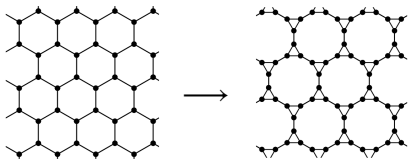

Since $\mathcal{G}'$ is also 3-regular, this process can be repeated indefinitely. In Theorem 4.3, we show that if the inequalities in (1) hold for $\mathcal{G}$, then they hold as strict inequalities for $\mathcal{G}'$.

Theorem 4.3. *Let $\mathcal{G}$ be a 3-regular planar lattice graph. If $\nu^{\Diamond}(\mathcal{G}) \le 2\pi\, z_{\mathcal{G}} \le \overline{\nu}(\mathcal{G})$, then*

$$\nu^{\Diamond}(\mathcal{G}') < 2\pi\, z_{\mathcal{G}'} < \overline{\nu}(\mathcal{G}').$$

Proof. By definition of $\mathcal{G}'$, $|VG'| = 3|VG|$. By [26, Theorem 4] with $r = 3, s = 1$,

$$z_{\mathcal{G}'} = \frac{1}{3} z_{\mathcal{G}} + \frac{1}{6} \log 15.$$

Recall $z_G^{\mathrm{fd}} = |VG| z_{\mathcal{G}}$. If we multiply the above equation for $z_{\mathcal{G}'}$ by $3|VG|$,

$$z_{G'}^{\mathrm{fd}} = z_G^{\mathrm{fd}} + \frac{|VG|}{2} \log 15.$$

We first prove the lower bound. Let F_n and F'_n denote the number of n–faces of G and G', respectively. By definition of $\mathcal{G}'$, $F'_{2n} = F_n$ and $F'_3 = |VG|$. Since G' is a 3-regular graph on a torus, $F' - E' + V' = 0$ and $3V' = 2E'$, hence $F' = E' - V' = V'/2 = 3|VG|/2$. Thus,

$$\#\{f \in FG' \,\big|\, |f| > 3\} = \frac{1}{2}|VG|.$$

Let $\Delta = \left(\mathrm{vol}^{\Diamond}(G') + \mathrm{vol}^{\Diamond}(G'^*)\right) - \left(\mathrm{vol}^{\Diamond}(G) + \mathrm{vol}^{\Diamond}(G^*)\right)$.

$$\begin{aligned}
\Delta = &\Big(\sum\nolimits_{\substack{f \in FG' \\ |f|>3}} \mathrm{vol}(B_{|f|}) \quad + \sum\nolimits_{\substack{f \in FG' \\ |f|=3}} \mathrm{vol}(B_3) \quad + \sum\nolimits_{v \in VG'} \mathrm{vol}(B_3) \Big) \\
&- \Big(\sum\nolimits_{f \in FG} \mathrm{vol}(B_{|f|}) \quad + \sum\nolimits_{v \in VG} \mathrm{vol}(B_3) \Big) \\
\hline
\Delta < &\ \frac{1}{2}|VG| \cdot 2\pi \log 2 \quad + |VG| \cdot 2v_{\mathrm{tet}} \quad + 2|VG| \cdot 2v_{\mathrm{tet}} \\
= &\ |VG|(\pi \log 2 + 6v_{\mathrm{tet}}).
\end{aligned}$$

The first inequality follows by Lemma 4.1 with $s = 2$ because $F'_{2n} = F_n$. Thus, since we assumed $\nu^{\Diamond}(\mathcal{G}) \le 2\pi\, z_{\mathcal{G}}$,

$$\begin{aligned}
\mathrm{vol}^{\Diamond}(G') + \mathrm{vol}^{\Diamond}(G'^*) &< \mathrm{vol}^{\Diamond}(G) + \mathrm{vol}^{\Diamond}(G^*) + |VG|(\pi \log 2 + 6v_{\mathrm{tet}}) \\
&\le 2\pi z_G^{\mathrm{fd}} + |VG|(\pi \log 2 + 6v_{\mathrm{tet}}) \\
&< 2\pi \left(z_G^{\mathrm{fd}} + \frac{|VG|}{2} \log 15 \right) \\
&= 2\pi z_{G'}^{\mathrm{fd}} \\
\nu^{\Diamond}(\mathcal{G}') &< 2\pi\, z_{\mathcal{G}'}.
\end{aligned}$$

The strict inequality follows because $(\pi \log 2 + 6v_{\mathrm{tet}}) < \pi \log 15$.

We now prove the upper bound, assuming $2\pi\, z_{\mathcal{G}} \le \overline{\nu}(\mathcal{G})$. Since $|EG'| = 3|EG|$, we have

$$\begin{aligned} z^{\mathrm{fd}}_{G'} &= z^{\mathrm{fd}}_{G} + \frac{|VG|}{2}\log 15 \\ &\le \frac{|EG|v_{\mathrm{oct}}}{2\pi} + \frac{|EG|}{3}\log 15 \\ &= |EG|\left(\frac{v_{\mathrm{oct}}}{2\pi} + \frac{\log 15}{3}\right) \\ &< 3|EG|v_{\mathrm{oct}}/2\pi \\ &= |EG'|v_{\mathrm{oct}}/2\pi \\ 2\pi\, z_{\mathcal{G}'} &< \overline{\nu}(\mathcal{G}'). \end{aligned}$$

The strict inequality follows because $\log 15 < 6v_{\mathrm{oct}}/2\pi$. □

4.3. Medial graph of a 3-regular planar lattice graph. For any 3-regular planar lattice graph $\mathcal{G}$, let $\mathcal{G}'$ be the medial graph of $\mathcal{G}$, which in this case is obtained by subdividing each edge once and then performing a $Y-\Delta$ transformation at every 3-valent vertex. The medial graph $\mathcal{G}'$ is 4-regular. For example, the Kagome lattice graph is the medial graph of the regular hexagonal lattice graph:

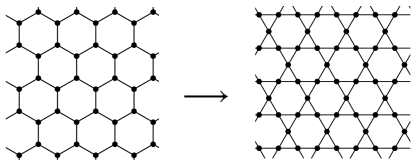

In Theorem 4.4, we show that if the lower bound in (1) holds for $\mathcal{G}$, then it holds with a strict inequality for $\mathcal{G}'$. In Corollary 4.5, we then apply Theorems 4.3 and 4.4 to obtain an infinite family of 4-regular planar lattice graphs for which both bounds in (1) hold with a strict inequality.

Theorem 4.4. *Let $\mathcal{G}$ be a 3-regular planar lattice graph. If $\nu^{\diamondsuit}(\mathcal{G}) \le 2\pi\, z_{\mathcal{G}}$, then $\nu^{\diamondsuit}(\mathcal{G}') < 2\pi\, z_{\mathcal{G}'}$.*

Proof. By definition of $\mathcal{G}'$, $|VG'| = |EG| = \frac{3}{2}|VG|$. By [26, Theorem 4] with $r = 3, s = 0$,

$$z_{\mathcal{G}'} = \frac{2}{3}z_{\mathcal{G}} + \frac{1}{3}\log 6.$$

We multiply this equation by $\frac{3}{2}|VG|$ to obtain

$$z^{\mathrm{fd}}_{G'} = z^{\mathrm{fd}}_{G} + \frac{|VG|}{2}\log 6.$$

Using the same notation as in the proof of Theorem 4.3, by definition of $\mathcal{G}'$, $F'_3 = |VG| + F_3$ and $F'_n = F_n$ for all $n \ne 3$.
Let $\Delta = \left(\mathrm{vol}^{\diamondsuit}(G') + \mathrm{vol}^{\diamondsuit}(G'^*)\right) - \left(\mathrm{vol}^{\diamondsuit}(G) + \mathrm{vol}^{\diamondsuit}(G^*)\right)$.

$$\begin{aligned}\Delta =&\Big(\sum\nolimits_{\substack{f\in FG'\\ |f|\neq 3}}\operatorname{vol}(B_{|f|})+\sum\nolimits_{\substack{f\in FG'\\ |f|=3}}\operatorname{vol}(B_3) \qquad +\sum\nolimits_{v\in VG'}\operatorname{vol}(B_4)\Big)\\ &-\Big(\sum\nolimits_{f\in FG}\operatorname{vol}(B_{|f|})+\sum\nolimits_{v\in VG}\operatorname{vol}(B_3)\Big)\end{aligned}$$

$$\begin{aligned}\Delta =&\ \big((|VG|+F_3)-F_3-|VG|\big)\operatorname{vol}(B_3) \qquad +|VG'|\operatorname{vol}(B_4)\\ =&\ \frac{3}{2}|VG|v_{\text{oct}}.\end{aligned}$$

Thus, since we assumed $\nu^{\Diamond}(\mathcal{G})\le 2\pi\, z_{\mathcal{G}}$,

$$\begin{aligned}\operatorname{vol}^{\Diamond}(G')+\operatorname{vol}^{\Diamond}(G'^{*}) &= \operatorname{vol}^{\Diamond}(G)+\operatorname{vol}^{\Diamond}(G^{*})+\frac{3}{2}|VG|v_{\text{oct}}\\ &\le 2\pi z_G^{\text{fd}}+\frac{3}{2}|VG|v_{\text{oct}}\\ &= 2\pi\left(z_G^{\text{fd}}+|VG|\frac{3v_{\text{oct}}}{4\pi}\right)\\ &< 2\pi\left(z_G^{\text{fd}}+\frac{|VG|}{2}\log 6\right)\\ &= 2\pi z_{G'}^{\text{fd}}\\ \nu^{\Diamond}(\mathcal{G}') &< 2\pi\, z_{\mathcal{G}'}.\end{aligned}$$

The strict inequality follows because $3v_{\text{oct}}<2\pi\log 6$. □

Corollary 4.5. *Let $\mathcal{G}_n$ denote the sequence of 3-regular planar lattice graphs obtained from the regular hexagonal lattice graph $\mathcal{G}_0=\mathcal{G}_{\hexagon}$ by truncation as in Theorem 4.3. Let $\mathcal{G}'_n$ be the 4-regular medial graph of $\mathcal{G}_n$ as in Theorem 4.4. Then $\nu^{\Diamond}(\mathcal{G}'_n)<2\pi\, z_{\mathcal{G}'_n}<\overline{\nu}(\mathcal{G}'_n)$ for all $n\ge 0$.*

Proof. The lower bound follows by Theorem 4.4. For the upper bound,

$$|VG_n|=2\cdot 3^n,\quad |VG'_n|=|EG_n|=3^{n+1},\quad |EG'_n|=2\cdot 3^{n+1}.$$

Applying the formulas in the proofs of Theorems 4.3 and 4.4,

$$\begin{aligned}z_{G'_n}^{\text{fd}} &= z_{G_{\hexagon}}^{\text{fd}}+\left(\sum\nolimits_{i=0}^{n-1}|VG_i|/2\right)\log 15+\frac{|VG_n|}{2}\log 6\\ &= \frac{10v_{\text{tet}}}{2\pi}+\left(\sum\nolimits_{i=0}^{n-1}3^i\right)\log 15+3^n\log 6\\ &= \frac{10v_{\text{tet}}}{2\pi}+\frac{3^n-1}{2}\log 15+3^n\log 6\\ &< 2\cdot 3^{n+1}v_{\text{oct}}/2\pi\\ &= |EG'_n|v_{\text{oct}}/2\pi\\ 2\pi\, z_{\mathcal{G}'_n} &< \overline{\nu}(\mathcal{G}'_n).\end{aligned}$$

The strict inequality follows because $\dfrac{10v_{\text{tet}}}{2\pi} - \log\sqrt{15} < 3^n\left(\dfrac{6v_{\text{oct}}}{2\pi} - \log 6\sqrt{15}\right)$ for all $n \geq 0$. □

5. Right-angled volume of a planar lattice graph

In this section, for dual simple 3–connected planar lattice graphs $\mathcal{G}$ and $\mathcal{G}^*$, we define another geometric invariant, which we call the right-angled volume $\text{vol}^\perp(\mathcal{G})$. We prove that Conjecture 1.1 implies that $\text{vol}^\perp(\mathcal{G}) \leq 2\pi\, z_{\mathcal{G}}$. We then prove the lower bound in Conjecture 1.1 for the regular planar lattice graphs using the isoradial dimer model.

An *orthogonal circle pattern* is a pair of circle packings whose contact graphs are planar dual graphs, such that dual edges are perpendicular and no other edges intersect; i.e., the tangent points of the dual circle packings coincide, and the two tangent lines at each point are perpendicular. The Koebe-Andreev-Thurston Circle Packing Theorem has been generalized to orthogonal circle patterns (see [15] and references therein): Every 3–connected plane graph admits an orthogonal circle pattern representation, which is unique up to Möbius transformations.

An *orthogonally dual embedding* of $\mathcal{G}$ and $\mathcal{G}^*$ is a planar embedding such that the inscribed circles in their faces form an orthogonal circle pattern. We will say that $\mathcal{G}$ and $\mathcal{G}^*$ are *orthogonally dual lattice graphs*, or that G and G^* are *orthogonally dual graphs* on the torus, if they admit an orthogonally dual embedding. Equivalently, the associated Temperleyan graph G^b is a quadrangulation embedded such that its faces are right kites, which are kites with at least two right angles, given by radii of the orthogonal circle pattern. Many well-known planar lattice graphs satisfy orthogonal duality; see Figure 6.

When lifted to the universal cover, considered as the plane at infinity for $\mathbb{H}^3$, this orthogonal circle pattern defines a right-angled biperiodic ideal hyperbolic polyhedron $\mathcal{P}$ in $\mathbb{H}^3$ whose vertices are the white vertices of $\mathcal{G}^b$. Let $P(G) = \mathcal{P}/\Lambda$, which is a hyperbolic polyhedron with finite volume. See Figure 7.

Definition 5.1. *If G and G^* are orthogonally dual graphs, define the* right-angled volume *of G and of $\mathcal{G}$ as*

$$\text{vol}^\perp(G) = 2\text{vol}(P(G)) \quad \textit{and} \quad \text{vol}^\perp(\mathcal{G}) = \frac{\text{vol}^\perp(G)}{|VG|}.$$

Note that $\text{vol}^\perp(G) = \text{vol}^\perp(G^*)$.

Theorem 5.2. *If G and G^* are dual simple 3–connected graphs on the torus with faces that are topologically disks, then*

(1) *G and G^* admit an orthogonally dual embedding on the torus, which is unique up to Möbius transformations,*
(2) *G and G^* are Tait graphs of an alternating link L in $T^2 \times I$, such that $(T^2 \times I) - L$ is hyperbolic,*
(3) $\text{vol}^\perp(G) \leq \text{vol}(G) \leq \text{vol}^\Diamond(G) + \text{vol}^\Diamond(G^*)$.

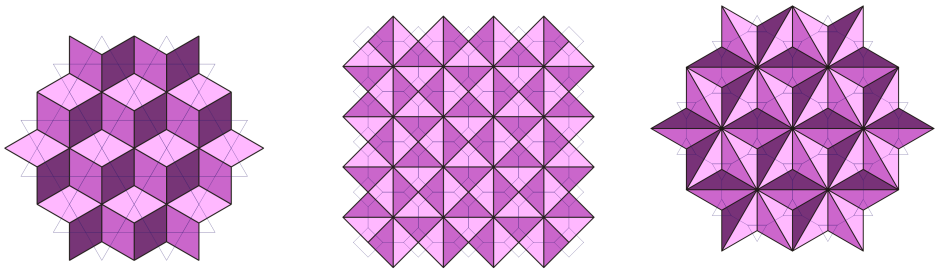

Lattice graph #4 Lattice graph #5 Lattice graph #7

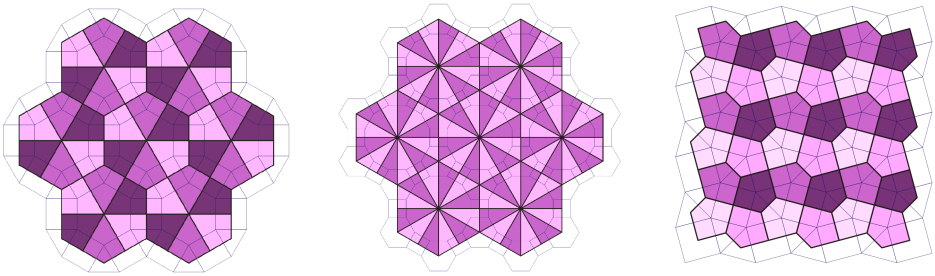

Lattice graph #8 Lattice graph #9 Lattice graphs #10,14

FIGURE 6. Lattice graphs $\mathcal{G}$ and $\mathcal{G}^*$ with orthogonally dual embeddings shown, so faces of $\mathcal{G}^b$ are right kites in each case. Labels from Table 1. Figures from [13].

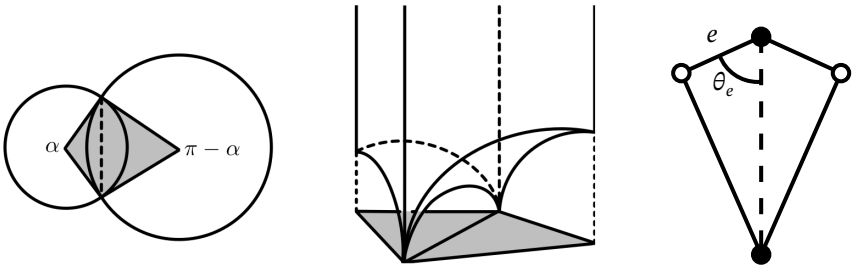

(a) (b) (c)

FIGURE 7. (a) A right kite formed by radii of intersecting orthogonal circles. (b) An ideal hyperbolic polyhedron bounded by vertical planes and intersecting hemispheres above the kite, which consists of two 3/4-ideal tetrahedra. (c) As a face of G^b, the kite has half-angle θ_e at edge e of G^b.

Proof. This theorem restates results from hyperbolic knot theory in [9, Theorem 7.5], and we explain the correspondence below. The proof relies on a result

about the existence of orthogonal circle patterns on the torus, due to Bobenko and Springborn [3].

The conditions on L in [9, Theorem 7.5] correspond to the following conditions on G and G^*:

(a) G and G^* are 2-connected; in particular, neither G nor G^* has loops,
(b) the faces of G and of G^* are topologically disks on the torus, and
(c) if $e_1, e_2 \in EG$ form a cut-set for G then a component of $EG \smallsetminus \{e_1, e_2\}$ is a path graph, and similarly for G^*.

Condition (a) means that L is reduced and weakly prime [9, Definition 7.1]; (b) means that L has a cellular emebedding on the torus; and (c) means that L has no cycle of tangles [9, Definition 6.2]. Finally, 3-connected graphs cannot have degree-2 vertices, so L has no bigons, which correspond to degree-2 vertices of G.

Our conditions on G and G^* imply the conditions (a), (b), (c). In particular, since edge-connectivity is at least vertex-connectivity, 3–connectedness precludes a two-edge cut as in (c). So the conditions in [9, Theorem 7.5] are satisfied by our conditions on G and G^*, which proves (1) and (2).

Since the projection of L is the medial graph of G,

$$\mathrm{vol}^{\diamondsuit}(L) = \sum_{f \in \{\text{faces of } L\}} \mathrm{vol}(B_{|f|}) = \mathrm{vol}^{\diamondsuit}(G) + \mathrm{vol}^{\diamondsuit}(G^*).$$

It remains to show that $\mathrm{vol}^{\perp}(L) = \mathrm{vol}^{\perp}(G)$. When the faces of G^b are right kites, the white vertices of G^b are the intersections of the orthogonal circle pattern, which correspond to crossings of L. The crossings of L are the vertices of the projection graph, and we can checkerboard color its faces. Thus, the orthogonal circle pattern given by inscribed circles of G and of G^* is exactly the orthogonal circle pattern given by the circumscribed circles of the shaded and unshaded faces of L. Thus, the right-angled polyhedron $P(G)$ is exactly $P(L)$ in the theorem, whose 1-skeleton is the projection graph of L. This proves (3). □

For example, the 3^3-4^2 lattice graph $\mathcal{G}$ is sometimes drawn as shown at left, but here is how to draw its orthogonally dual embedding:

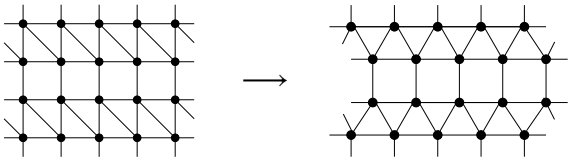

By Theorem 5.2, for planar lattice graphs $\mathcal{G}$ that satisfy orthogonal duality,

$$\mathrm{vol}^{\perp}(\mathcal{G}) \le \mathrm{vol}(\mathcal{G}) \le \nu^{\diamondsuit}(\mathcal{G}).$$

Moreover, as we did for $\nu^{\diamondsuit}(\mathcal{G})$, we can compute $\mathrm{vol}^{\perp}(\mathcal{G})$ using only the local geometry of its orthogonally dual embedding. If G and G^* are orthogonally dual, then the right kite angles of G^b are uniquely determined. For $e \in EG^b$, let $2\theta_e$ be the angle swept out counter-clockwise around the black vertex of e

to the adjacent edge, which is one of the vertex angles of a right kite. Then θ_e will be called the half-angle at e, as shown in Figure 7(c). The chord shown in Figure 7(a) is the diagonal of a right kite joining the white vertices of G^b. If $v \in VG$ and $v' \in VG^*$ are the black vertices of the kite, then it has sides $e, e' \in EG^b$, such that $2\theta_e + 2\theta_{e'} = \pi$. Let $L(\theta)$ be the Lobachevsky function, as in Definition 2.1. By Milnor's volume formula, the volume of the two 3/4-ideal tetrahedra shown in Figure 7(b) is $L(\theta_e) + L(\theta_{e'})$. Therefore,

$$\mathrm{vol}^{\perp}(G) = \sum_{e \in EG^b} 2L(\theta_e). \tag{2}$$

For a regular planar lattice graph $\mathcal{G}$, the lower bound in Conjecture 1.1 was proved with equality using number theory in [7, Theorems 12, 13]. Below we give another proof using the toroidal dimer model and the fact that $\mathcal{G}$ satisfies both orthogonal duality and a geometric condition called an *isoradial embedding*. Namely, $\mathcal{G}$ is embedded isoradially in the plane if each face is inscribed in a circle of radius 1 whose center is in the interior of that face. Such an isoradial embedding is equivalent to a rhombic embedding of an associated quadrangulation by joining each vertex of $\mathcal{G}$ with the circumcenter of every face incident to that vertex. Equivalently, G^b is embedded such that its black vertices are vertices of the rhombi, and its white vertices are centers of the rhombi.

Theorem 5.3. *For the regular planar lattice graphs, $\mathcal{G}_{\triangle}$, $\mathcal{G}_{\square}$, $\mathcal{G}_{\hexagon}$,*

$$\mathrm{vol}^{\perp}(G) = \mathrm{vol}(G) = \mathrm{vol}^{\diamondsuit}(G) + \mathrm{vol}^{\diamondsuit}(G^*) = 2\pi\, \mathrm{m}(p(z,w)) = 2\pi\, z_G^{\mathrm{fd}}.$$

Thus, the lower bound in Conjecture 1.1 holds with equality.

Proof. The toroidal dimer model is a statistical mechanics model of the set of dimer coverings of $G^b = \mathcal{G}^b/\Lambda$. The characteristic polynomial of the dimer model is defined as $p(z,w) = \det \kappa(z,w)$, where $\kappa(z,w)$ is the Kasteleyn matrix. Let $G_n^b = \mathcal{G}^b/(n\Lambda)$ be the finite balanced bipartite toroidal graph, and $Z(G_n^b)$ be the number of dimer coverings of G_n^b. By [20], its entropy is given by

$$\lim_{n\to\infty} \frac{1}{n^2} \log Z(G_n^b) = \mathrm{m}(p(z,w)). \tag{3}$$

See [7] for details, examples and references.

For an isoradial graph, critical edge weights are defined as $\nu(e) = 2\sin\theta_e$, where edge e is the diagonal of a rhombus and θ_e is the half-angle at e. Thus, $\nu(e)$ is the length of the other diagonal of the rhombus, which is dual to e. The function ν is called the critical weight function for the isoradial dimer model on G^b, introduced in [19]. By [12], in the isoradial case with the critical edge weights, the entropy of the toroidal dimer model can be computed using only the local geometry of the isoradial embedding:

$$2\pi\, \mathrm{m}(p_\nu(z,w)) = 2\pi \lim_{n\to\infty} \frac{1}{n^2} \log Z(G_n^b, \nu) = \sum_{e \in EG^b} \big(2\theta_e \log(2\sin\theta_e) + 2L(\theta_e)\big). \tag{4}$$

We emphasize two key differences between equations (3) and (4): First, edges in equation (3) do not have the critical edge weights because we are interested in counting spanning trees. Second, the Mahler measure $\mathrm{m}(p(z,w))$ in equation (3) cannot be expressed using Lobachevsky functions as in equation (4); see [7] for exact computations of $\mathrm{m}(p(z,w))$.

We now use that each $\mathcal{G}$ satisfies both orthogonal duality and isoradiality. Let v be a black vertex of G^b; i.e., $v \in VG \cup VG^*$. Let $2\theta_i$ be the angle between adjacent edges e_i, e_{i+1} of G^b incident to v. When $\theta_i = \theta$ for all i at some $v \in VG \cup VG^*$, then all edges incident to v have the same critical weight $2\sin\theta$, which can be factored out of the Kasteleyn matrix. This factor appears as the summand $\log(2\sin\theta)$ in $\mathrm{m}(p_v(z,w))$; i.e., $\mathrm{m}(p_v(z,w)) = \mathrm{m}(p(z,w)) + \log(2\sin\theta)$. Moreover, in this case $\theta_i = \pi/|v|$ for all i, so

$$\begin{aligned} 2\pi \log(2\sin\theta) &= 2\pi \log\left(\frac{1}{|v|}\sum_{i=1}^{|v|} 2\sin\theta_i\right) = \sum_{i=1}^{|v|} 2\theta_i \log(2\sin\theta_i) \\ &= \sum_{e\in EG^b} 2\theta_e \log(2\sin\theta_e). \end{aligned}$$

Since this occurs at every $v \in VG \cup VG^*$ for the regular planar lattice graphs, we have

$$\begin{aligned} 2\pi\,\mathrm{m}(p(z,w)) &= 2\pi\big(\mathrm{m}(p_v(z,w)) - \log(2\sin\theta)\big) \\ &= 2\pi\,\mathrm{m}(p_v(z,w)) - \sum_{e\in EG^b} 2\theta_e \log(2\sin\theta_e) = \sum_{e\in EG^b} 2L(\theta_e) \\ &= \mathrm{vol}^{\perp}(G). \end{aligned}$$

The last equality is by equation (2). Moreover, since $\mathrm{vol}(B_n) = 2n\,L(\pi/n)$,

$$\begin{aligned} \sum_{e\in EG^b} 2L(\theta_e) &= \sum_{v\in VG\cup VG^*}\sum_{i=1}^{|v|} 2L(\theta_i) = \sum_{v\in VG\cup VG^*} 2|v|\,L\Big(\frac{\pi}{|v|}\Big) \\ &= \sum_{v\in VG\cup VG^*} \mathrm{vol}(B_{|v|}) = \mathrm{vol}^{\diamondsuit}(G) + \mathrm{vol}^{\diamondsuit}(G^*). \end{aligned}$$

Therefore, by Theorem 5.2,

$$\mathrm{vol}^{\perp}(G) = \mathrm{vol}(G) = \mathrm{vol}^{\diamondsuit}(G) + \mathrm{vol}^{\diamondsuit}(G^*) = 2\pi\,\mathrm{m}(p(z,w)).$$

Finally, $\mathrm{m}(p(z,w)) = z_G^{\mathrm{fd}}$ essentially by equation (3), as explained in [6, Proposition 5.3]. When we divide by $|VG|$, the lower bound in Conjecture 1.1 holds with equality for $\mathcal{G}$. □

Remark 5.4. In [19], Kenyon interpreted the Lobachevsky functions as the volume of a hyperbolic polyhedron $\mathcal{P}$ associated to $(\mathcal{G}^b)^*$, using the circle pattern given by circumcircles of the faces of $(\mathcal{G}^b)^*$. Vertices of $(G^b)^*$ are the intersections of a circle pattern whose radii are the edges of rhombi. When lifted to the universal cover, considered as the plane at infinity for $\mathbb{H}^3$, this circle pattern defines a biperiodic ideal hyperbolic polyhedron $\mathcal{P}$ in $\mathbb{H}^3$ whose vertices are the

vertices of $(\mathcal{G}^b)^*$. Let $\mathtt{P} = \mathcal{P}/\Lambda$, which is a hyperbolic polyhedron with finite volume.

If G has an isoradial embedding, and $\mathtt{P}$ is the hyperbolic polyhedron associated to $(G^b)^*$, then

$$\mathrm{vol}(\mathtt{P}) = \sum_{e \in EG^b} 2L(\theta_e) \;\leq\; \mathrm{vol}^{\Diamond}(G) + \mathrm{vol}^{\Diamond}(G^*).$$

The first equality was proved in [19]. For the inequality, we can decompose $\mathtt{P}$ into tetrahedra, and collect them around each black vertex of G^b to form a bipyramid. This is possible because around each vertex v, $\sum \theta_e = \pi$ for all edges e incident to v. By [1], the maximal volume of hyperbolic bipyramids is achieved by the regular bipyramids, whose volumes sum to $\mathrm{vol}^{\Diamond}(G)+\mathrm{vol}^{\Diamond}(G^*)$.

When G is isoradial, the circles that determine $\mathtt{P}$ are all congruent, which is not required to bound a hyperbolic polyhedron. On the other hand, the polyhedron $P(G)$ given by an orthogonal circle pattern is right-angled, which is another special case. The geometry for these two types of planar lattice graphs corresponds as follows:

	$\mathcal{G}$ and $\mathcal{G}^*$ satisfy orthogonal duality	$\mathcal{G}$ and $\mathcal{G}^*$ satisfy isoradiality
Circle pattern:	orthogonal inscribed circles	isoradial circumscribed circles
Local geometry:	G^b-faces are right kites	black VG^b form rhombi
Hyperbolic polyhedron:	vertices of P are white VG^b	vertices of $\mathtt{P}$ are $V(G^b)^*$
Volume of polyhedron:	$\mathrm{vol}(P) = \sum_{e \in EG^b} L(\theta_e)$	$\mathrm{vol}(\mathtt{P}) = \sum_{e \in EG^b} 2L(\theta_e)$
Volume bound:	$2\mathrm{vol}(P) \leq \mathrm{vol}^{\Diamond}(G) + \mathrm{vol}^{\Diamond}(G^*)$	$\mathrm{vol}(\mathtt{P}) \leq \mathrm{vol}^{\Diamond}(G) + \mathrm{vol}^{\Diamond}(G^*)$

References

[1] ADAMS, COLIN Bipyramids and bounds on volumes of hyperbolic links. *Topology Appl.* **222** (2017), 100–114. MR3630197 doi: 10.1016/j.topol.2017.03.002 1151, 1152, 1157, 1158, 1168

[2] ADAMS, COLIN; FLEMING, THOMAS; LEVIN, MICHAEL; TURNER,ARI M. Crossing number of alternating knots in $S \times I$. *Pacific J. Math.* **203** (2002), no. 1, 1–22. MR1895923 doi: 10.2140/pjm.2002.203.1 1148

[3] BOBENKO, ALEXANDER; SPRINGBORN, BORIS Variational principles for circle patterns and Koebe's theorem. *Trans. Amer. Math. Soc.* **356** (2004), no. 2, 659–689. MR2022715 doi: 10.1090/S0002-9947-03-03239-2 1165

[4] BUCHIN, KEVIN; SCHULZ, ANDRÉ On the number of spanning trees a planar graph can have. Algorithms—ESA 2010. Part I, Lecture Notes in Comput. Sci., vol. 6346, *Springer, Berlin*, 2010, 110–121. MR2762847 doi: 10.1007/978-3-642-15775-2_10 1156

[5] BURTON, STEPHAN D. The determinant and volume of 2-bridge links and alternating 3-braids. *New York J. Math.* **24** (2018), 293–316. MR3778507 1157

[6] CHAMPANERKAR, ABHIJIT; KOFMAN, ILYA Determinant density and biperiodic alternating links. *New York J. Math.* **22** (2016), 891–906. MR3548129 1155, 1167

[7] CHAMPANERKAR, ABHIJIT; KOFMAN, ILYA; LALÍN, MATILDE Mahler measure and the vol-det conjecture. *J. Lond. Math. Soc. (2)* **99** (2019), no. 3, 872–900. MR3977894 doi: 10.1112/jlms.12200 1148, 1149, 1150, 1152, 1153, 1155, 1156, 1157, 1166, 1167

[8] CHAMPANERKAR, ABHIJIT; KOFMAN, ILYA; PURCELL, JESSICA S. Geometrically and diagrammatically maximal knots. *J. Lond. Math. Soc. (2)* **94** (2016), no. 3, 883–908. MR3614933 doi: 10.1112/jlms/jdw062 1149, 1153, 1157

[9] ———, Geometry of biperiodic alternating links. *J. Lond. Math. Soc. (2)* **99** (2019), no. 3, 807–830. MR3977891 doi: 10.1112/jlms.12195 1151, 1152, 1164, 1165

[10] CHANG, SHU-CHIUAN; WANG, WENYA Spanning trees on lattices and integral identities. *Journal of Physics A: Mathematical and General* **39** (2006), no. 33, 10263–10275. MR2256591 doi: 10.1088/0305-4470/39/33/001 1155

[11] CULLER, MARC; DUNFIELD, NATHAN; GOERNER, MATTHIAS; WEEKS, JEFFREY R. SnapPy, a computer program for studying the geometry and topology of 3-manifolds. Available at http://snappy.computop.org. 1148, 1155

[12] DE TILIÈRE, BÉATRICE Partition function of periodic isoradial dimer models. *Probab. Theory Related Fields* **138** (2007), no. 3-4, 451–462. MR2299715 doi: 10.1007/s00440-006-0041-2 1166

[13] DOROZINKSI, TADEUSZ (USER:TED-43) https://commons.wikimedia.org/wiki/Category:Semiregular_tilings_with_overlaid_dual_(violet) (2009). 1164

[14] EGOROV, ANDREI; VESNIN, ANDREI The Vol-Det Conjecture for highly twisted alternating links. *Math Notes* **119** (2026), 21–28. 1157

[15] FELSNER, STEFAN; ROTE, GÜNTER On primal-dual circle representations. 2nd Symposium on Simplicity in Algorithms, SOSA 2019, January 8-9, 2019, San Diego, CA, USA (Jeremy T. Fineman and Michael Mitzenmacher, eds.), OASIcs, vol. 69, *Schloss Dagstuhl - Leibniz-Zent. Inform., Wadern* (2019), pp. 8:1–8:18. MR3904984 1163

[16] GAN, HONG-CHUAN Bipyramid volume, Mahler measure and some $\mathbb{Z}^2$-periodic links. arXiv:2202.10218 (2022). 1149

[17] HOWIE, JOSHUA A.; PURCELL, JESSICA S. Geometry of alternating links on surfaces. *Trans. Amer. Math. Soc.* **373** No. 4 (2020), 2349–2397. MR4069222 doi: 10.1090/tran/7929 1148

[18] KAPLAN-KELLY, R. Right-angled links in thickened surfaces. *Geom Dedicata* **218** 113 (2024). MR4817704 doi: 10.1007/s10711-024-00960-w 1153

[19] KENYON, R. The Laplacian and Dirac operators on critical planar graphs. *Invent. Math.* **150** (2002), no. 2, 409–439. MR1933589 doi: 10.1007/s00222-002-0249-4 1166, 1167, 1168

[20] KENYON, R.; OKOUNKOV, A.; SHEFFIELD, S. Dimers and amoebae. *Ann. of Math. (2)* **163** (2006), no. 3, 1019–1056. MR2215138 doi: 10.4007/annals.2006.163.1019 1148, 1155, 1156, 1166

[21] KENYON, R.; PROPP, J.; WILSON, D. Trees and matchings. *Electron. J. Combin.* **7** (2000), Research Paper 25, 34 pp. MR1756162 doi: 10.37236/1503 1148

[22] LI, SHULI; YAN, WEIGEN Spanning trees and dimer problem on the Cairo pentagonal lattice. *Applied Mathematics and Computation* **337** (2018), 34–40. MR3827595 doi: 10.1016/j.amc.2018.05.012 1155

[23] LYONS, RUSSELL Asymptotic enumeration of spanning trees. *Combin. Probab. Comput.* **14** (2005), no. 4, 491–522. MR2160416 doi: 10.1017/S096354830500684X 1148, 1156, 1157

[24] RUEN, TOM (USER:TOMRUEN), Euclidean tilings by convex regular polygons, https://en.wikipedia.org/wiki/Euclidean_tilings_by_convex_regular_polygons. 2015. 1154, 1155

[25] TEMPERLEY, H.N.V. Combinatorics: Proceedings of the British Combinatorial Conference 1973, London Math. Soc. Lecture Notes Series, vol. 13, 1974, pp. 202–204. 1147

[26] TEUFL, E.; WAGNER, S. On the number of spanning trees on various lattices. *J. Phys. A* **43** (2010), no. 41, 415001, 8. MR2726685 doi: 10.1088/1751-8113/43/41/415001 1149, 1154, 1158, 1160, 1161

(Abhijit Champanerkar) DEPARTMENT OF MATHEMATICS, COLLEGE OF STATEN ISLAND & THE GRADUATE CENTER, CITY UNIVERSITY OF NEW YORK, NEW YORK, NY 10016, USA
achampanerkar@gmail.com

(Ilya Kofman) DEPARTMENT OF MATHEMATICS, COLLEGE OF STATEN ISLAND & THE GRADUATE CENTER, CITY UNIVERSITY OF NEW YORK, NEW YORK, NY 10016, USA
Ilya.Kofman@csi.cuny.edu

This paper is available via http://nyjm.albany.edu/j/2026/32-46.html.